

# RSC Advances



This is an *Accepted Manuscript*, which has been through the Royal Society of Chemistry peer review process and has been accepted for publication.

*Accepted Manuscripts* are published online shortly after acceptance, before technical editing, formatting and proof reading. Using this free service, authors can make their results available to the community, in citable form, before we publish the edited article. This *Accepted Manuscript* will be replaced by the edited, formatted and paginated article as soon as this is available.

You can find more information about *Accepted Manuscripts* in the [Information for Authors](#).

Please note that technical editing may introduce minor changes to the text and/or graphics, which may alter content. The journal's standard [Terms & Conditions](#) and the [Ethical guidelines](#) still apply. In no event shall the Royal Society of Chemistry be held responsible for any errors or omissions in this *Accepted Manuscript* or any consequences arising from the use of any information it contains.

# Preparation and properties of thermally conductive polyimide/boron nitride composites

Na Yang<sup>1</sup>, Chen Xu<sup>1</sup>, Jun Hou<sup>1</sup>, Yanmei Yao<sup>1</sup>, Qingxin Zhang<sup>1</sup>, Maryam E. Grami<sup>2</sup>, Lianqi He<sup>3</sup>, Nongyue Wang<sup>1</sup>, Xiongwei Qu<sup>1\*</sup>

1 Institute of Polymer Science and Engineering, School of Chemical Engineering, Hebei University of Technology, Tianjin, P. R. China, 2 Composite Materials Engineering, Winona State University, Winona, Minnesota, USA, 3 Ouya Hose Corporation, Heshui, Hebei, P. R. China

**Abstract:** Polyimide (PI) has been widely used as the preferred packaging matrix materials due to its low dielectricity, outstanding insulation and excellent thermal stability. Hexagonal boron nitride (*h*-BN) microparticles were functionalized with silane coupling agent, 3-glycidyloxypropyltrimethoxy silane ( $\gamma$ -MPS), to improve the interface action with the PI matrix. The modified *h*-BN (*m*-BN) particles were used to fabricate the PI/*m*-BN composites with enhanced thermal conductivity by in-situ polymerization. The Fourier transform infrared (FTIR) spectra, thermo-gravimetric analysis (TGA), transmission electron microscopy (TEM) and contact angle test proved that  $\gamma$ -MPS coupling agent molecules had been chemically grafted onto the *h*-BN surface. In addition, the effects of the *m*-BN content on thermal conductivity of PI/*m*-BN composites were investigated. The composite obtained with 40 wt% *m*-BN particles loading presented a thermal conductivity of 0.748 W/(m·K), 4.6 times higher than that of pure PI. Meanwhile, the fabricated PI/*m*-BN composites kept excellent electrical insulation and thermal stability. The glass transition temperature values of the PI/*m*-BN composites decreased slightly while the storage modulus improved with the increase of *m*-BN content. These results showed that PI/*m*-BN composites may offer new applications in microelectronic industry because the future substrate materials require effective heat dissipation.

**Keywords:** polyimide, boron nitride, composite, surface modification, thermal conductivity, morphology

## INTRODUCTION

Along with the rapid development of science, technology and worldwide economy, the electrical materials have been unable to meet the requirements to dissipate the emitting heat because of their increasing integration. As polymer materials have the advantages of excellent electrical resistivity, fatigue resistance, good chemical resistance and easy processing, they are progressively utilized in aerospace, packaging matrix materials, electronic information, heat engineering and other fields. But the thermal conductivity of traditional polymeric materials is generally low, most falls in between 0.1 and 0.25 W/(m·K),<sup>1-2</sup> which limits their widely use as thermal conductive materials in industry.<sup>3</sup> Therefore, polymer composites with high thermal conductivity and electrically insulating properties have attracted increasing interests to solve heat-dissipation problems.

To date, two methods are used to improve thermal conductivity of polymer materials. One is to synthesize intrinsic thermal conductive polymer materials with  $\pi$ -conjugated bond, which heat conduction is via the electronic heat conduction mechanism or the phonon mechanism for heat conduction by improving the

\* Corresponding authors: Xiongwei Qu ([xwqu@hebut.edu.cn](mailto:xwqu@hebut.edu.cn))

crystallization of polymer.<sup>4,5</sup> This method is used fewer because of its preparation and processing complexity. The other alternative method is to introduce high thermal conductivity fillers into the polymer matrix. Electrically conductive fillers such as traditional carbon materials (diamond,<sup>6</sup> grapheme,<sup>7,8</sup> carbon nanotubes<sup>9</sup>), and metal particles<sup>10</sup> have a high intrinsic thermal conductivity of 2000-3000 W/(m·K)<sup>11</sup> and are more promising for increasing the thermal conductivity of composites. This method can only be used in the fields that do not require high electrical insulation. Therefore, high thermal conductivity with insulating ceramic fillers, such as aluminum nitride (AlN),<sup>12</sup> alumina (Al<sub>2</sub>O<sub>3</sub>),<sup>13</sup> silica (SiO<sub>2</sub>),<sup>14</sup> boron nitride (BN)<sup>15</sup> have been widely adopted to prepare high thermal conductivity and electric insulation polymer composites. In addition, the loading content, size, surface treatment of inorganic fillers and the interact interface with the matrix will influence the performance of thermal conductivity.

Recently, hexagonal boron nitride (*h*-BN) has attracted increasing attention due to its high intrinsic thermal conductivity, excellent electrical insulation, and low dielectric constant. It has a structure like graphite, which boron and nitrogen atoms are positioned alternatively to form 2-D conjugated layers.<sup>16</sup> The thermal conductivity of boron nitride along the basal plane (001) is up to 300 W/(m·K), which makes BN as a reasonable candidate to prepare well-balanced composites with high thermal conductivity and electrical insulation properties. Nevertheless, the interfacial compatibility between inorganic fillers and polymer matrix is very poor due to the difference in the surface polarity, which results in inorganic fillers hardly homogeneous dispersion in the polymer matrix and causes agglomeration phenomenon. Therefore, surface modification is necessary to improve the interface action between BN particles and polymer matrix. Many modified methods, such as chemical grafting method and physisorption have been used to improve the wettability and dispersion of BN particles, and to increase thermal conductivity of the composites. Jin synthesized a new organized BN to significantly increase amount amine groups by introducing isocyanate on the surface of BN.<sup>17</sup> Yu adopted the method that hyperbranched aromatic polyamide was grafted onto the surface of BN to achieve strong interface action and desirable dispersion.<sup>18</sup> Lee and Kuo groups attempted to use BN particles precoated with polyimide (PI) to improve the thermal conductivity of the composites.<sup>19,20</sup> On the other hand, for polyimide matrix composites, researchers mainly focused on BN nanoparticle<sup>21-23</sup>. Li et al. prepared PI/BN composites by adding 3-mercaptopropionic acid (MPA)-modified fillers with different nano-sized particles.<sup>21</sup> Diahm identified that BN nano-particle size had a strong influence on the thermal conduction of PI.<sup>22</sup> The dielectric properties of polyimide/boron nitride (PI/BN) nanocomposite films were investigated as a function of the BN nanofiller size.<sup>23</sup> As the dispersibility of micro inorganic particles in polymer is better than nanofillers, therefore micro *h*-BN particles were used as fillers in this work. Silane coupling agent has been widely used to functionalize or modify the silicon-containing surfaces, such as glass fibers and fillers. Because of which not only can form a monomolecular layer on inorganic filler surfaces to improve the wettability and dispersion of inorganic fillers, but also they are easily got and of low price. So in this work, the silane coupling agent of 3-glycidyloxypropyltrimethoxy silane ( $\gamma$ -MPS) was introduced to functionalize the surface of BN particles to enhance the interfacial affinity and dispersibility of BN particles. A series of PI composites with *h*-BN and *m*-BN particles were prepared by in-situ polymerization. The thermal conductivity, insulating property, morphology and

molecular movement of the PI/*m*-BN composites with different *m*-BN contents were investigated. Meanwhile there was an interesting phenomenon that the glass transition temperature values of the PI/*m*-BN composites decreased slightly as the *m*-BN fillers increased, which was different from previous reports that inorganic particles filled polymer resins.<sup>11,21,24</sup> In order to explain this new phenomenon, we study the effect of the imidization degree on the structure of the PI/*m*-BN composites. As far as we know, it has not been reported before. By appropriate selection of functionalized BN, the PI/*m*-BN composites have the potential in modern electronic devices requiring both high heat resistance and high thermal conductivity.

## EXPERIMENTAL

### *Materials*

Pyromellitic dianhydride (PMDA, purity $\geq$ 98.5%, Sinopharm Chemical Reagent Co., China) and 4,4'-oxydianiline (ODA, purity $\geq$ 98%, Aladdin Chemistry Co., China) were dried in a vacuum oven at 120°C for 12 h. Anhydrous dimethylacetamide (DMAc), toluene, sulfuric acid, nitric acid and ethanol were purchased from Tianjin Fuchen Chemical Co., China. DMAc and toluene were purified with molecular sieves to remove water before used. Sulfuric acid, nitric acid and ethanol were used without further purification. Hexagonal boron nitride (*h*-BN) particles (purity $\geq$ 99.0%, 3~5 $\mu$ m) were bought from Qingzhou Materials Co., China, and were dried in a vacuum at 80°C for 12h. The silane coupling agent, 3-glycidyloxypropyltrimethoxy silane ( $\gamma$ -MPS), was provided by Aladdin Chemistry Co., China, and used as received.

### *Surface modification of h-BN*

The *h*-BN particles were treated ultrasonically at 250 W for 9 h in a 100 ml mixed solution that nitric acid and sulfuric acid volume ratio was 1:3. Then the suspension was magnetically stirred with reflux condensation in an 80°C oil bath for 72 h to increase the hydroxide functional groups on the surface of *h*-BN particles. After the treatment, the *h*-BN particles were washed with deionized water for several times until the filtrated water was neutral, dried at 60°C under vacuum overnight. *h*-BN particles were modified with a silane coupling agent, 3-glycidyloxypropyltrimethoxy silane ( $\gamma$ -MPS). 1 g of BN particles and 0.02 g  $\gamma$ -MPS were dispersed in 100 ml dry toluene in a 250 ml three-necked flask, equipped with a magnetic stirrer and a reflux condenser. The mixture was refluxed at 115°C under N<sub>2</sub> for 9 h. *h*-BN particles were then rinsed with absolute ethyl alcohol for three times, and dried under vacuum at 80°C for 24 h to get  $\gamma$ -MPS-modified *h*-BN (*m*-BN).

### *Preparation of PI/BN composites*

Two-step method was used to prepare PI/*m*-BN composites with different *m*-BN contents. The synthesized procedure is shown in Figure 1. First of all, a certain amount of *m*-BN (0, 1, 3, 5, 8, 10, 20, 30 and 40% on the weight ratio of PI matrix) was charged in 20 ml DMAc with ultrasonic dispersion at 250 W for 1 h. Then 1.2 g (6 mmol) ODA was added into a 100ml three-necked round-bottom flask equipped with a mechanical stirrer, and the dispersion was stirred at room temperature under N<sub>2</sub> until ODA was thoroughly dissolved. 1.307g (6 mmol) PMDA was added into the above dispersion every 0.5 h for three times, and then stirred for 8 h at room temperature to form a homogeneous viscous composite precursor, polyamic acid/*m*-BN (PAA/*m*-BN) pulp. Finally, the pulp was cast on a glass plate by a doctor's knife and placed in a vacuum oven at 60°C for 7 h to remove the

solvent. The second step was thermally imidization process. The film was further thermally treated in muffle furnace by stepwise heating, from room temperature to 100, 150, 200, 250°C, and 300°C, each temperature maintaining for 60 min to convert the PAA to PI completely. The PI/*m*-BN composite films were cooled to room temperature and peeled off from glass surface by immersing in distilled water. The thickness of the film was controlled about 100 μm. In addition, the reference composites with the addition of untreated BN (*h*-BN) were also synthesized and denoted as PI/*h*-BN.

### Characterization

Fourier-transform infrared (FT-IR) spectroscopy was conducted with a Bruker Vector-22 instrument ranging from 4000 to 400 cm<sup>-1</sup>. Thermal gravimetric analyses (TGA) were performed with a SDT Q600 (TA Instruments, USA) from 25 to 800°C at a heating rate of 10°C under the nitrogen atmosphere. The X-ray diffraction (XRD) analysis was carried out on a Smart Lab X-ray diffraction spectrometer equipped with Cu Ka radiation at a 2θ angle of 10-80° as well as at an operating voltage of 40 kV and a current of 30 mA. Transmission electron microscopy (TEM, Leica EM, Germany) was used to observe the morphology for *h*-BN and *m*-BN particles. The wettability characteristics of BN particles were performed on a Kruss tensiometer (DAS30, Germany). Dynamic mechanical analyzer (DMA) was performed on a DMA Q800 (TA Instruments, USA) in a tensile mode under N<sub>2</sub>. Samples were measured from room temperature to 450°C at a heating rate of 10°C/min and a frequency of 1Hz. The morphology and dispersion of *m*-BN particles in the PI matrix were investigated by a field emission scanning electron microscopy (FE-SEM, Nova Nano SEM 450, FEI). The fractured surfaces of composites were sputtered with a layer of gold before scanning to avoid charge accumulation. Thermal conductivity of PI/*h*-BN composite was measured by TC 3000 Series Thermal Conductivity Apparatus (Xi'an Xiayi Co. Ltd., China) based on the transient hot-wire technique at room temperature. Each sample was tested five times to insure accuracy of the measurement, and thermal conductivity ( $\lambda$ , W/(m·K)) was calculated by the following equation:

$$\lambda = \frac{q}{4\pi(d\Delta T / d \ln t)}$$

Where,  $q$  is the heat generation conducted by per unit per unit length of the wire,  $\Delta T$  is the temperature changes of the wire and  $t$  is the measuring time.<sup>25</sup> The ultrahigh electric resistor (ZC36, Shanghai Sixth Electric Meter Factory, China) was used to measure volume and surface resistivity of PI/*m*-BN composites at room temperature.

## RESULT AND DISCUSSION

### Modification on the surfaces of *h*-BN particles

It is important for the composites to enhance the dispersion and interface action between the inorganic filler particles and the polymer matrix. Samples mixing untreated *h*-BN particles with PI matrix may result in agglomeration of *h*-BN particles, which will influence the thermal transport performance of the composites. In order to improve the compatibility between the PI and the *h*-BN particles, 3-glycidyloxypropyltrimethoxy silane ( $\gamma$ -MPS) was used as a surface modifier to functionalize the surface of *h*-BN particles. The FTIR spectra of *h*-BN and  $\gamma$ -MPS-modified *h*-BN (*m*-BN) are shown in Figure 2. In the curve of *h*-BN particles, the broad absorption peak around 1375 cm<sup>-1</sup> was owing to the in-plane stretching vibration of *h*-BN, and the peak at 818 cm<sup>-1</sup> was

related to out-of-plane bending absorption of the B-N-B. The broad absorption band at  $3442\text{ cm}^{-1}$  was originated from amino group or hydroxyl group (-OH) stretching at the edge planes on the *h*-BN surface, which was the reactive group from the coupling agent. The new peaks near  $2920\text{ cm}^{-1}$  and  $2846\text{ cm}^{-1}$  were attributed to asymmetric and symmetric  $-\text{CH}_2-$  stretching vibrations from  $\gamma$ -MPS. The peaks appear at  $1103\text{ cm}^{-1}$  and  $1020\text{ cm}^{-1}$  were a fingerprint of the presence of Si-O bonds, which resulted from the reaction between the hydroxylated *h*-BN and the silane surfactant. These changes of characteristic peaks confirmed that the silane coupling agent,  $\gamma$ -MPS, had been successfully grafted onto the surfaces of *h*-BN particles.

Thermal gravimetric analysis (TGA) was further used to illustrate the successful modification on *h*-BN particles' surfaces. Figure 3 shows the TGA curves of *h*-BN and *m*-BN. Raw *h*-BN and *m*-BN both showed some differences in weight loss with the temperature. Compared with raw *h*-BN particles, the *m*-BN had a relatively large weight loss at temperatures around  $350^\circ\text{C}\sim 450^\circ\text{C}$ , which was attributed to the decomposition of the silane molecules. The TGA results were in consistent with that of FTIR, i.e. the silane coupling agent,  $\gamma$ -MPS, had been chemically grafted on the surface of *h*-BN particles as the *m*-BN sample was extracted with boiling toluene for two days before analyzing. While the weight grafting ratios is relatively low, the possible reason may be that the morphology of *h*-BN is similar to graphite, the 001 basal plane is very smooth and has no surface functional groups available for chemical bonding or interaction. Only the edge planes of the lamellar structure have a small quantity of functional groups such as amino groups or hydroxyl groups.<sup>26</sup> This result is further proved by TEM images of the *h*-BN and *m*-BN particles, as shown in Figure 4. It can be seen that the 001 basal plane of *h*-BN is very smooth and almost no uneven edges (Figure 4(a)), while they becomes rough on the surface of *m*-BN after the modification (Figure 4(b)).

XRD technique is a method to characterize the crystallite size and three-dimensional order of materials. XRD patterns of *h*-BN and *m*-BN are shown in Figure 5. Apparently, the crystal structure of *h*-BN particles did not change after the surface modification because there was no new peaks appeared. For raw *h*-BN, the peaks at around  $2\theta=26.9^\circ$  and  $41.7^\circ$  were attributed to the diffraction of (002) and (100) planes of *h*-BN, respectively. The thickness of *c* axis direction ( $L_c$ ) of *h*-BN can be calculated from the (002) peak using Sherrer's equation, as follows:

$$L_c = \frac{k\lambda}{\beta \cos \theta}$$

Where,  $\lambda$  is the wavelength of the radiation,  $0.154056\text{ nm}$ ,  $\beta$  is the full width at half maximum,  $\theta$  is the Bragg's angle of (002) peak,  $k$  is a constant,  $0.89$ .<sup>27</sup> The  $L_c$  values of *h*-BN particles before and after modification were calculated as  $30.36\text{ nm}$  and  $29.44\text{ nm}$ , respectively, stating the value of  $L_c$  has no significant change, that is, the samples have a perfectly ordered structure. The perfect order structure is very important to form thermally conductive network of the composites.

Meanwhile, the surface wettability properties of raw and modified BN were investigated by water contact angle measurement. Related contact angle images are shown in Figure 6. Raw *h*-BN belongs to a polar filler, stronger hydrophilic with a contact angle of  $53.5^\circ$  (Figure 6(a)). After the surfaces were modified with a silane coupling agent ( $\gamma$ -MPS), the contact angle increased to  $99.3^\circ$  (Figure 6(b)) because of the introduction of alkyl groups, that

was, improved the hydrophobic property and promoted the dispersity of *m*-BN particles in PI matrix.

#### ***Thermal conductivity of the PI/*m*-BN composites***

The thermal conductivity of PI/*m*-BN composites with different weight ratios was measured by the transient hot-wire method at room temperature. Figure 7 presents the results of the PI/BN composites with *h*-BN and *m*-BN particles. It can be seen that the thermal conductivity of the composites increased with the addition of BN. The pure PI had a relatively low thermal conductivity of 0.168 W/(m·K). When the loading level of *m*-BN particles increased to 40 wt%, a significant enhancement of the thermal conductivity could be seen, 0.748 W/(m·K), 4.5 times higher than that of pure PI. Two factors are responsible for increasing the thermal conductivity of PI/*m*-BN composites. One is the filler content. For the composites with relatively low BN loading, there is no direct contact with each other between BN particles. This is due to the BN particles isolated and wrapped dispersion in PI matrix, which leads to the interface thermal resistance between *h*-BN particles becoming very large. Therefore, the values of thermal conductivity of composites filled with low BN contents are low. With increasing of the BN content, the BN particles could contact with each other to form continuous chains of particles over the whole samples and form thermally conductive pathways or thermal percolating network. The thermal conductivity of PI/*m*-BN composites is improved further after the modification of *h*-BN surface which results from the higher interface compatibility between *m*-BN particles and PI matrix. In theory, the thermal conductive pathways are formed by the interface of the composites through phonon boundary scattering.<sup>28</sup> The silane coupling agent acts as phonon transfer bridges between *m*-BN particles and the PI matrix. One end is linked with the surface of the *m*-BN fillers and the other of the carboxyl group reacts with the end of PAA main chain. The surface chemistry modification could promote *m*-BN particles dispersing well in the PI matrix, and reduce the interfacial thermal resistance caused by phonon scattering. The strong covalent bonds between the *m*-BN particles and PI matrix improve interfacial compatibility. Figure 8 shows the fractured surfaces of the composites with different *m*-BN contents by SEM observation. Figure 8(a) shows that fractured surface of pure PI is very smooth. When the content of *m*-BN particles is 5wt% (Figure 8(b)), *m*-BN particles are separated from each other and disperse uniformly in the PI matrix. While the content of *m*-BN particles increases to 20wt% and 40wt% (Figure 8(c-d)), the particles contact each other and form conductive pathways in composites, resulting in high thermal conductivity of the composites.

#### ***Thermal stability of the PI/*m*-BN composites***

Thermal stability is one of the important properties for the composites in processing and application. Addition of fillers into a polymer matrix may bring some changes in the thermal characteristics of the resulting composites. Figure 9 shows the TGA curves for PI/*m*-BN composites with different *m*-BN contents. The temperatures at 10wt% mass loss and the maximum degradation rate are listed in Table 1. It can be seen that pure PI exhibited high thermal stability, and the temperatures for 10% weight loss ( $T_{10\%}$ ) and maximum degradation rate temperature ( $T_{\max}$ ) appeared at 585.5°C and 598.7°C, respectively. This is attributed to the existence of benzene rings and imide rings of polyimide. While the  $T_{10\%}$  values of the PI/*m*-BN composites increased with increasing of the *m*-BN content, and the  $T_{\max}$  values of composites were all higher than that of pure PI. This is due to that *m*-BN particles possess high heat capacity and thermal conductivity and can form heat resisting layers acting as mass transport barriers, which will delay the escape of volatile degradation.<sup>29</sup> As a result, the *m*-BN particles leads to

the enhanced thermal stability of the PI/*m*-BN composites.

#### ***Electrical insulation property of the PI/*m*-BN composites***

The electrical insulation property is important for thermally conductive packaging materials, which are used in the fields of electron and electrical appliance. High electrical insulation is a key factor to ensure safety and stability work of the electronic components. Surface resistivity and volume resistivity are two of the crucial parameters that characterize the electrical insulation property. Figure 10 shows the electrical insulation property of PI/*m*-BN composites for different *m*-BN contents. The results suggested that the volume resistivity of pure PI was about  $4.2 \times 10^{17} \Omega$ , and the volume resistivity of composites decreased slightly with *m*-BN introduction, while still maintained the same order of magnitude as the pure PI. Meanwhile the surface resistivity displays no change. The composites still possess excellent electrical insulation property. Therefore, the PI/*m*-BN composites kept high thermal conductivity with fine electrical insulation properties, and are appropriate for the application as packaging materials.

#### ***Dynamic mechanical analysis of the PI/*m*-BN Composites***

Dynamic mechanical analysis (DMA) is a useful technique to obtain the characteristic parameters of the materials in the structure, process and application. For inorganic fillers filled polymer composites, the viscoelasticity not only reflects the every component's molecular relaxation but also reveals the morphology, the interactions among each component and other factors of the composites.<sup>30</sup> The storage moduli ( $E'$ ) as a function of temperature for PI/*m*-BN composites are plotted in Figure 11(a). It is clearly observed that the storage moduli of the composites are obviously higher than that of the pure PI within the experimental temperature range, and the PI composite filled with a larger content of *m*-BN particles has a higher storage modulus value. For example, the storage moduli of the PI/*m*-BN composites with 0%, 10%, 20%, 30% and 40wt% *m*-BN contents at 150°C were 1710, 1982, 2503, 4215 and 4573 MPa, respectively. This phenomenon can be explained in terms of the addition of the *m*-BN fillers. The *m*-BN particles possess inherent high modulus and their large diameter-thickness ratio makes the existence of bigger interfacial interaction between the *m*-BN particles and PI matrix. This leads to the applied stress transferred from the PI to *m*-BN fillers. When the temperature is above 380°C, the storage modulus decreased significantly, this is because that the molecular chains need to dissipate energy in order to overcome viscous motion.

The loss tangent ( $\tan \delta$ ) is the ratio of loss modulus to the storage modulus. The width and height of  $\tan \delta$  peak are important for measuring the damping behavior of materials. The temperature of the  $\tan \delta$  maximum peak is regarded as the glass transition temperature ( $T_g$ ). Figure 11(b) shows the variation of  $\tan \delta$  as a function of temperature for PI/*m*-BN composites. It is interesting to note that the  $T_g$  values of the composites shifted to lower temperatures with the addition of *m*-BN particles. The  $T_g$  values of PI/*m*-BN composites with 0%, 10%, 20%, 30%, 40wt% *m*-BN contents are 417.5, 412.2, 409.6, 408.9, 404.4°C, respectively, as listed in Table 1. Nevertheless, for polyimide composites, some researchers reported an increase in the  $T_g$  as a function of filler content,<sup>21,31</sup> however, decreases in the  $T_g$  have rarely been reported. What result in the  $T_g$  decrease? Firstly, the addition of rigid *m*-BN particles occupy a certain part of volume, and the molecular chain accumulation intensity decreases, leading to the motion of polymer chain segments much easier. The weak chain-chain interaction results in a lower  $T_g$  value.<sup>8</sup> Secondly, the imidization degree of polyimide would reduce with the introduction of *m*-BN particles, leading to



the decrease of  $T_g$ . Because PI with a higher degree of imidization has stiff molecular chains and thus reduces molecular motion ability, on the contrary, the molecular chains of PI/*m*-BN composites with a lower degree of imidization show higher flexible.<sup>32</sup> This is described in more detail below. Thirdly, the *h*-BN particles were functionalization by silane coupling agent, a number of flexible silane chain-segments formed on the BN surface increased the molecular chains segmental mobility of PI, and thus led to a reduction in  $T_g$  of PI/*m*-BN composites.<sup>33</sup> The height of the  $\tan \delta$  peak gradually decreased with increasing *m*-BN particles, indicating the rigidity of composites increased. This is related to the strong interfacial interaction between *m*-BN particles and PI matrix.

#### ***Effect of the imidization degree on the structure of the PI/*m*-BN composites***

FTIR spectroscopy can effectively evaluate the imidization degree and chemical structure of PI/*m*-BN composites. In this study, the imidization degree was evaluated by FTIR spectroscopy based on absorbance superposition and Lambert-Beer Law.<sup>34</sup> FTIR spectra of the *m*-BN, PI and PI/*m*-BN composites are shown in Figure 12. The absorption peak at  $1497\text{cm}^{-1}$  related to the C-C stretching of aromatic benzene is designated as an internal standard because it does not change during imidization process. The degree of imidization can be determined by the ratio of the absorbance at  $1371\text{ cm}^{-1}$  (C-N-C) to that of C-C stretching at  $1497\text{ cm}^{-1}$ , namely  $I_{1371}/I_{1497}$ .<sup>35</sup> The values calculated by  $I_{1371}/I_{1497}$  of the PI/*m*-BN composites with 0%, 10%, 20%, 30%, 40wt% *m*-BN contents were 0.77, 0.74, 0.67, 0.66, 0.55, respectively (Table 1). It can be seen that the imidization degree gradually decreased with the increasing of *m*-BN content. It is likely because the inorganic-organic networks are formed in the composites after the addition of *m*-BN particles, which result from the stereo-hindrance effect. It will restrict the PAA chain segments convert into PI chain segments. Furthermore, the addition of *m*-BN particles can result in the molecular weight of PI/*m*-BN composites lower than that of PI. The small molecules in PI/*m*-BN composites can absorb energy and transfer it to heat capacity, while PI with high molecular weight may prevent the heat capacity to be lost from its surface.<sup>36</sup> So with the *m*-BN content increasing, the imidization degree of composites decreased, leading to the reduction in  $T_g$  of PI/*m*-BN composites. The peaks at  $815\text{ cm}^{-1}$  and  $1370\text{ cm}^{-1}$  become broader due to *m*-BN absorption, as shown in Figure 12.

XRD results further illustrated the stability of crystal structure of *m*-BN. Figure 13 compares the XRD patterns of PI/*m*-BN composites. The diffraction peak at around  $15^\circ$  to  $19^\circ$  indicates the amorphous structure of PI molecules, and the diffraction peak intensity become stronger and broader when the *m*-BN contents increased from 10% to 40%. This showed that the addition of *m*-BN particles destroyed the orderly arrangement of PI and lowered the packing density of PI molecules. Meanwhile, the patterns of the PI/*m*-BN composites were similar to that of *h*-BN, indicating that *m*-BN particles still remained stable after being added into the PI matrix.<sup>37</sup> The XRD peak intensity at  $2\theta=26.9^\circ$  increased with the addition of the higher *m*-BN mass fractions, while the *d*-spacing of the layer distance of *m*-BN in the PI/*m*-BN composites show slight change which might be due to the BN aggregates in the PI matrix.<sup>38</sup>

## **CONCLUSIONS**

PI/*m*-BN composites were successfully prepared via in situ polymerization. The silane coupling agent, namely,

3-glycidyoxypropyltrimethoxy silane ( $\gamma$ -MPS), was used to modify raw *h*-BN, and acted as a bridge between *m*-BN particles and PI matrix. FTIR analysis, contact angle test and TEM observation demonstrated that the silane coupling agent was chemically grafted on the surfaces of *h*-BN particles. This improved dispersion of *m*-BN particles in PI matrix and increased the thermal conductivity of PI/*m*-BN composites. When the loading level of *m*-BN reached 40%, the thermal conductivity of 0.768 W/(m·K) was obtained, which was 4.6 times higher than that of pure polyimide. Meanwhile, the SEM observation showed that *m*-BN particles uniformly dispersed in PI matrix, and particles contacted with each other to form a continuous thermal conductive network, contributing to the enhancement of thermal conductivity of the composites. In addition, the thermal stability, storage modulus was higher than that of pure PI except to the decrease of  $T_g$  value with the addition of *m*-BN into PI matrix. Besides, the PI/*m*-BN composites maintained excellent electrical insulation property, which has promising applications in microelectronic industry as future substrate materials requiring effective heat dissipation.

## ACKNOWLEDGMENTS

This work was financially supported by National Natural Science Foundation (contact no. 51573037), Program for Changjiang Scholars and Innovative Research Team in University (IRT13060) and Key Lab for Micro- and Nano-Scale Boron Nitride Materials in Hebei Province.

## REFERENCES

- [1] Y.M. Chen, J.M. Ting, *Carbon*, 2002, **40**, 359.
- [2] L.L. Qin, G.H. Li, J. Hou, *Polym. Compos.*, 2015, **36**, 1675.
- [3] M. Hu, D. Yu, J. Wei, *Polym. Test.*, 2007, **26**, 333.
- [4] C.L. Choy, Y.W. Wong, G.W. Yang, *J. Polym. Sci. Polym. Phys.*, 1999, **37**, 3359.
- [5] M. Akatsuka, Y. Takezawa, *J. Appl. Polym. Sci.*, 2003, **89**, 2464.
- [6] J. Che, T. Çağın, W. Deng, *J. Chem. Phys. A.*, 2000, **113**, 6888.
- [7] S. Ghosh, W. Bao, D.L. Nika, S. Subrina, *Nat. Mater.*, 2010, **9**, 555.
- [8] M.H. Tsai, I.H. Tseng, J.C. Chiang, J.J. Li, *ACS Appl. Mater. Inter.*, 2014, **6**, 8639.
- [9] Z. Han, A. Fina, *Prog. Polym. Sci.*, 2011, **36**, 914.
- [10] Y.P. Mamunya, V.V. Davydenko, P. Pissis, E.V. Lebedev, *Eur. Polym. J.*, 2002, **38**, 1887.
- [11] J. Hou, G.H. Li, N. Yang, *RSC Adv.*, 2014, **4**, 44282.
- [12] S. Kume, I. Yamada, K. Watari, *J. Am. Ceram. Soc.*, 2009, **92**, S153.
- [13] L. Fang, C. Wu, R. Qian, *RSC Adv.*, 2014, **4**, 21010.
- [14] Y. Liao, X. Wu, H. Liu, *Thermochim. Acta.*, 2011, **526**, 178.
- [15] K. Wattanakul, H.M. and N. Yanumet, *J. Appl. Polym. Sci.*, 2011, **119**, 3234.
- [16] E. Çakmakçı, C. Koçyiğit, S. Cakır, A. Durmus, *Polym. Compos.*, 2014, **35**, 530.
- [17] W. Jin, W. Zhang, Y. Gao, *Appl. Surf. Sci.*, 2013, **270**, 561.
- [18] J. Yu, X. Huang, C. Wu, *Polymer*, 2012, **53**, 471.
- [19] H.L. Lee, O.H. Kwon, S.M. Ha, *Phys. Chem. Chem. Phys.*, 2014, **16**, 20041.
- [20] D.H. Kuo, C.Y. Lin, Y.C. Jhou, J.Y. Cheng, G.S. Liou, *Polym. Compos.*, 2013, **34**, 252.

- [21] T.L. Li, S.L.C. Hsu, *J. Phys. Chem. B.*, 2010, **114**, 6825.
- [22] S. Diahm, F. Saysouk, M.L. Locatelli, B. Belkerk, *J. Appl. Polym. Sci.*, 2015, **132**, 42461.
- [23] S. Diahm, F. Saysouk, M.L. Locatelli, T. Lebey, *J. Phys. D: Appl. Phys.*, 2015, **48**, 385301.
- [24] R. Qian, J. Yu, L. Xie, *Polym. Advan. Technol.*, 2013, **24**, 348.
- [25] W. Yu, S.U.S. Choi, *Rev. Sci. Instrum.*, 2006, **77**, 76102-76102-3.
- [26] K. Sato, H. Horibe, *J. Mater. Chem.*, 2010, **20**, 2749.
- [27] X.B. Huan, W. Wei, X.L. Zhao, *Chem. Commun.*, 2010, **46**, 8848.
- [28] S.Y. Yang, C.C.M. Ma, C.C. Teng, Y.W. Huang, *Carbon*, 2010, **48**, 592.
- [29] Y.S. Ye, Y.C. Yen, C.C. Cheng, Y.J. Syu, *Polymer*, 2010, **51**, 430.
- [30] G.D. Smith, D. Bedrov, L. Li, *J. Chem. Phys. A.*, 2002, **117**, 9478.
- [31] F.X. Qiu, Y.M. Zhou, J.Z. Liu, *Eur. Polym. J.*, 2004, **40**, 713.
- [32] M.B. Saeed, M.S. Zhan, *Eur. Polym. J.*, 2006, **42**, 1844.
- [33] H.C. Wu, M.R. Kessler, *ACS Appl. Mater. Inter.*, 2015, **7**, 5915.
- [34] Y.K. Xu, M.S. Zhan, K. Wang, *J. Polym. Sci. Pol. Phys.*, 2004, **42**, 2490.
- [35] W.S. Li, Z.X. Shen, J.Z. Zheng, S.H. Tang, *Appl. Spectrosc.*, 1998, **52**, 985.
- [36] Y.H. Lu, M.S. Zhan, *J. Polym. Sci. Poly. Phys.*, 2005, **43**, 3621.
- [37] S.K. Kisku, S.K. Swain, *J. Am. Ceram. Soc.*, 2012, **95**, 2753.
- [38] A. Alias, Z. Ahmad, A.B. Ismail, *Mat. Sci. Eng. R.*, 2011, **176**, 799.

## Tables

Table 1 Thermal stability, dynamic mechanical properties and imidization degree of PI/*m*-BN composites with different *m*-BN contents

sample	TGA		DMA			FTIR
	$T_{10\%}$ (°C)	$T_{\max}$ (°C)	$T_g$ (°C)	Tan $\delta$	$E'$	$I_{1371}/I_{1497}$
PI/0% <i>m</i> -BN	585.5	598.7	417.5	0.3212	1710	0.77
PI/10% <i>m</i> -BN	592.0	603.7	412.2	0.2569	1982	0.74
PI/20% <i>m</i> -BN	595.2	601.1	409.6	0.2481	2503	0.67
PI/30% <i>m</i> -BN	596.5	600.9	408.9	0.2144	4215	0.66
PI/40% <i>m</i> -BN	603.4	605.1	404.4	0.1947	4573	0.55

## Figure captions

Figure 1 Procedure of preparing PI/*m*-BN composites.

Figure 2 FTIR curves of *h*-BN, *m*-BN and the silane modifier ( $\gamma$ -MPS).

Figure 3 TGA curves of *h*-BN and *m*-BN measured in N<sub>2</sub>.

Figure 4 TEM micrographs of particles: (a) *h*-BN and (b) *m*-BN.

Figure 5 XRD patterns of *h*-BN and *m*-BN.

Figure 6 Contact angle between water and hybrid fillers, (a) *h*-BN, (b) *m*-BN.

Figure 7 Thermal conductivity of the PI/BN composites as a function of BN content.

Figure 8 SEM images of the fractured surface of samples: (a) pure PI, and PI/*m*-BN composites with different *m*-BN contents, (b) 5wt%, (c) 20wt%, (d) 40wt%.

Figure 9 TGA thermal degradation curves of the PI/*m*-BN composites.

Figure 10 Electrical insulation properties of PI/*m*-BN composites as a function of *m*-BN content.

Figure 11 Storage modulus (a) and loss tangent (b) versus temperature for PI/*m*-BN composites with different *m*-BN contents.

Figure 12 FTIR spectra of (1) *m*-BN, (2) PI and PI/*m*-BN composites with different *m*-BN contents: (3) 10%, (4) 20%, (5) 30%, (6) 40%.

Figure 13 XRD patterns of (a) Pure PI, *m*-BN and PI/*m*-BN composites with different *m*-BN contents, (b) Enlarge (a) of the 2 $\theta$  ranging from 26° to 28°.

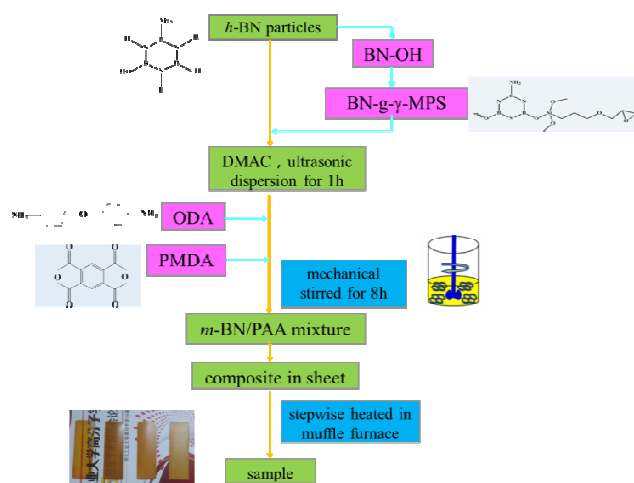


Figure 1 Procedure of preparing PI/*m*-BN composites.

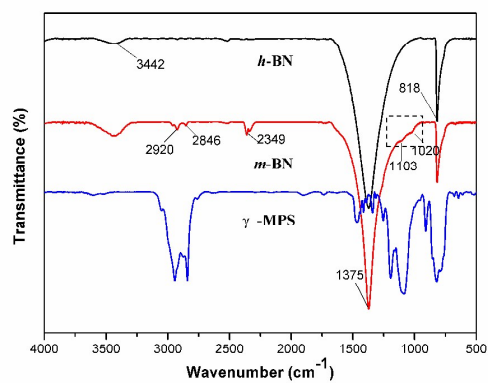


Figure 2 FTIR curves of *h*-BN, *m*-BN and the silane modifier ( $\gamma$ -MPS).

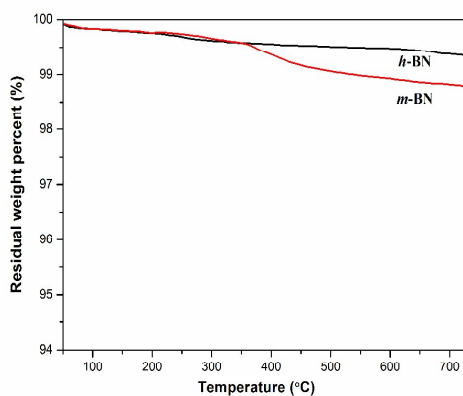


Figure 3 TGA curves of *h*-BN and *m*-BN measured in  $\text{N}_2$ .

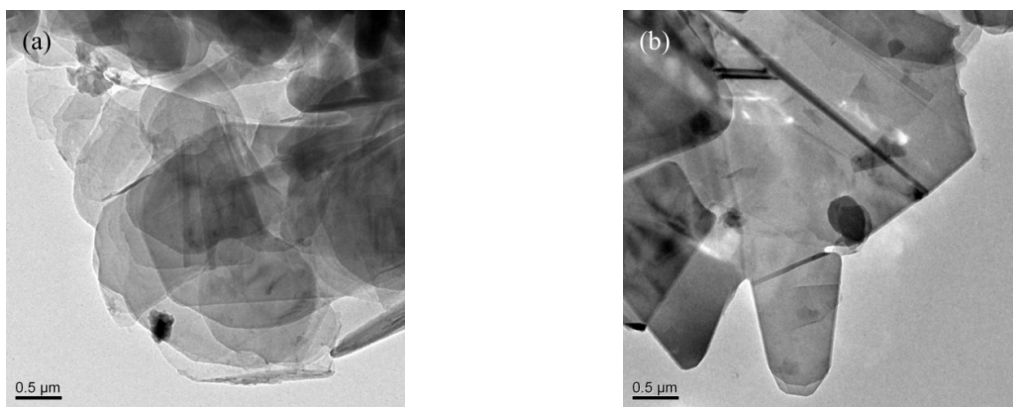


Figure 4 TEM micrographs of particles: (a) *h*-BN and (b) *m*-BN.

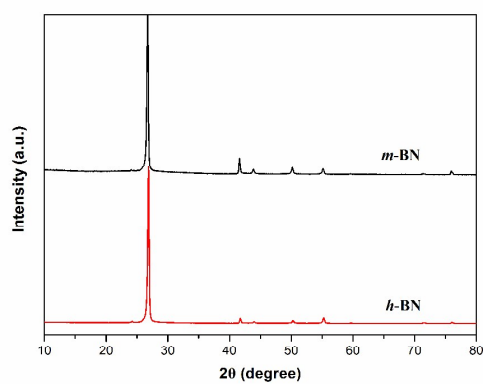


Figure 5 XRD patterns of *h*-BN and *m*-BN.

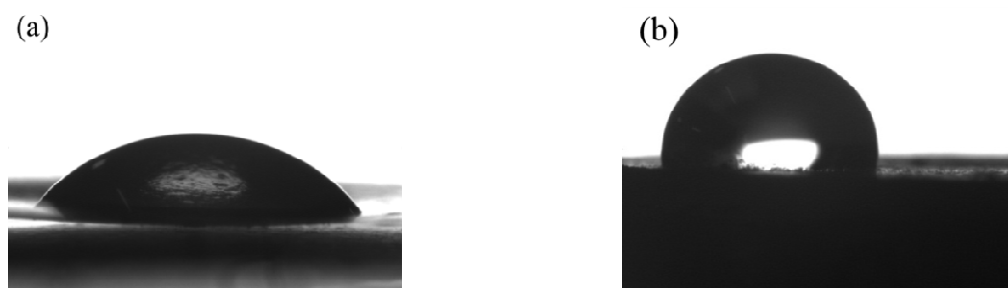


Figure 6 Contact angle between water and hybrid fillers, (a) *h*-BN, (b) *m*-BN.

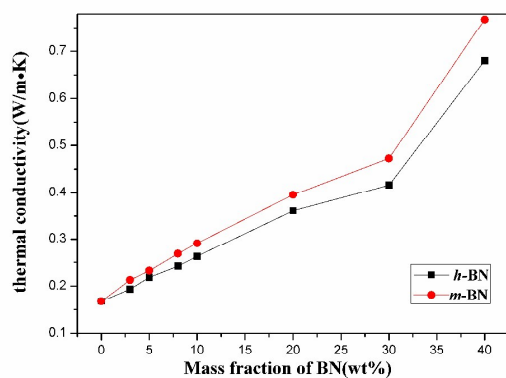


Figure 7 Thermal conductivity of the PI/BN composites as a function of BN content.

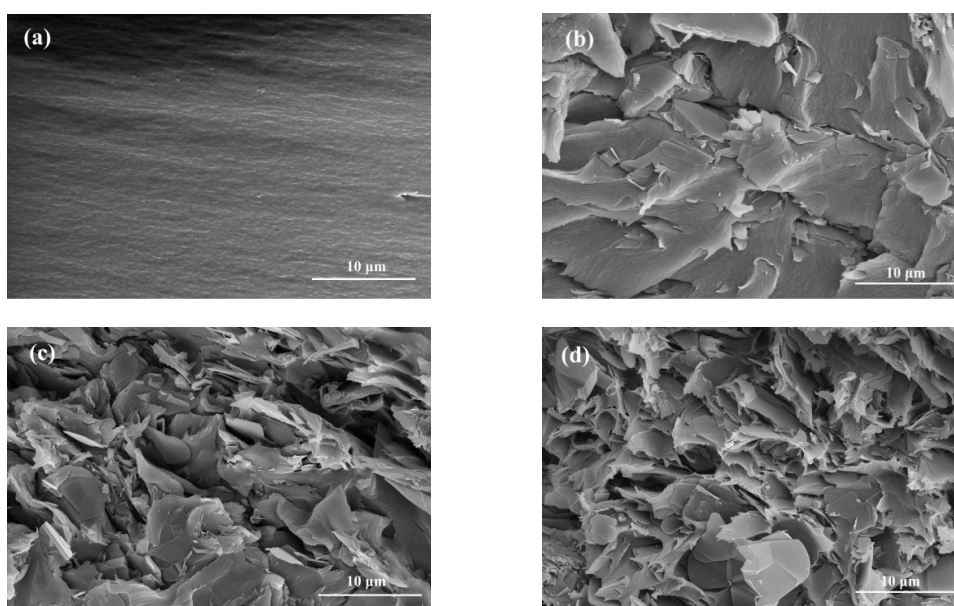


Figure 8 SEM images of the fractured surface of samples: (a) pure PI, and PI/*m*-BN composites with different *m*-BN contents, (b) 5wt%, (c) 20wt%, (d) 40wt%.

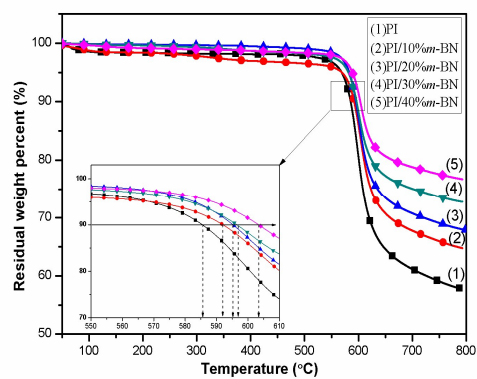


Figure 9 TGA thermal degradation curves of PI/*m*-BN composites.

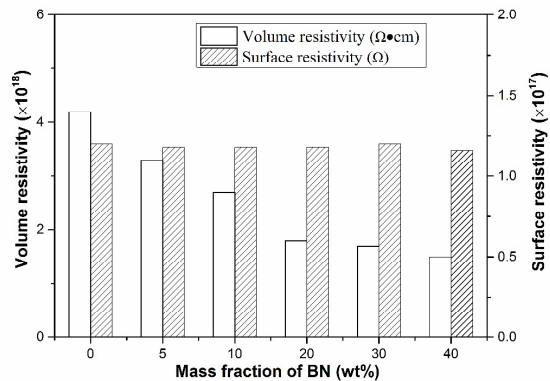


Figure 10 Electrical insulation properties of PI/*m*-BN composites as a function of *m*-BN content.

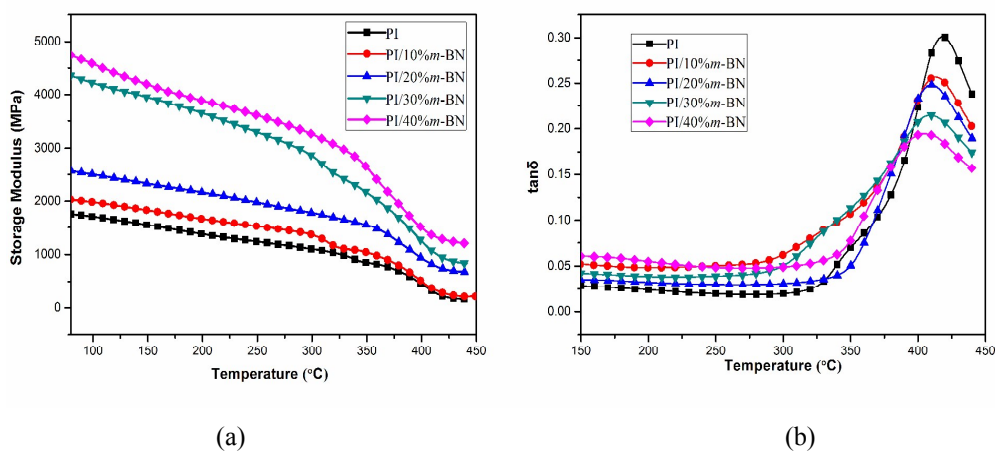


Figure 11 Storage modulus (a) and loss tangent (b) versus temperature for PI/*m*-BN composites with different *m*-BN contents.

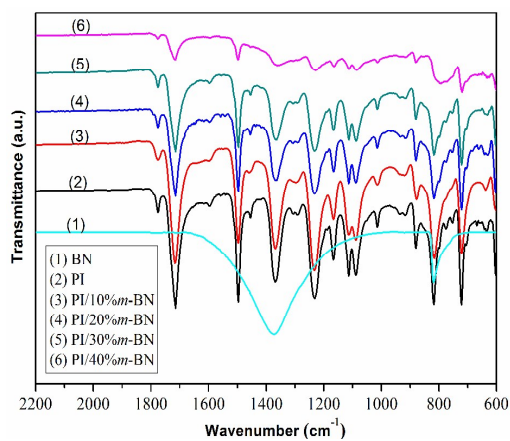


Figure 12 FTIR spectra of (1) *m*-BN, (2) PI and PI/*m*-BN composites with different *m*-BN contents: (3) 10%, (4) 20%, (5) 30%, (6) 40%.



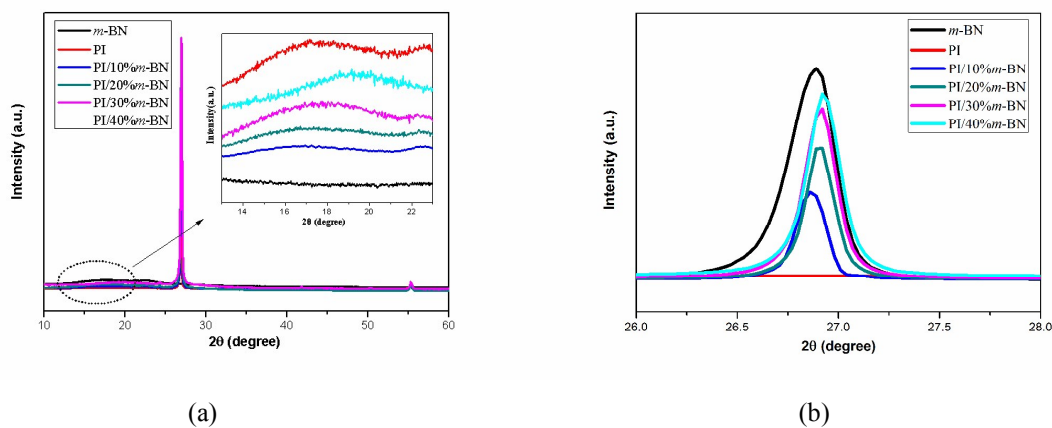
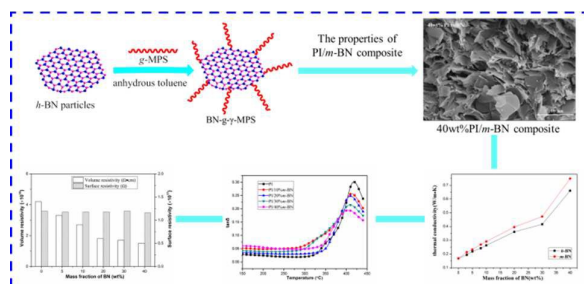


Figure 13 XRD patterns of (a) Pure PI, *m*-BN and PI/*m*-BN composites with different *m*-BN contents, (b) Enlarge (a) of the  $2\theta$  ranging from  $26^\circ$  to  $28^\circ$ .

## Graphical Abstract



Hexagonal boron nitride (*h*-BN) micro particles functionalized by silane coupling agent, 3-glycidyloxypropyltrimethoxy silane ( $\gamma$ -MPS), were used to fabricate polyimide/BN composites. The thermal conductivity of the composites with 40wt% *m*-BN content was increased to 0.748 W/(m·K), 4.5 times higher than that of the pure PI, which may offer new applications in microelectronic industry.